The Substrate Reaction Mechanism of Class III Anaerobic Ribonucleotide Reductase

Kyung-Bin Cho,[†] Fahmi Himo,[‡] Astrid Gräslund,[†] and Per E. M. Siegbahn*[,§]

Department of Biophysics, The Arrhenius Laboratories, Stockholm University, SE-106 91 Stockholm, Sweden, Department of Molecular Biology, The Scripps Research Institute, 10550 N. Torrey Pines Rd., La Jolla, California 92037, and Department of Physics, Stockholm University, Box 6730, SE-113 85 Stockholm, Sweden

Received: February 28, 2001; In Final Form: April 20, 2001

The substrate mechanism of class III anaerobic ribonucleotide reductase has been studied using quantum chemical methods. The study is based on the previously suggested mechanism for the aerobic class I enzyme, together with the recently determined X-ray structure of the anaerobic enzyme. The initial steps are similar in the mechanisms of these enzymes, but for the suggested rate-limiting steps there are key differences. In the class I enzyme, the 3′-keto group of the substrate is protonated in a step involving formation of a sulfur−sulfur bond between two cysteines. One of these cysteines is not present in the anaerobic enzyme. Instead, carbon dioxide is formed in this step from formate, which is present as a cofactor. In line with previous suggestions from experimental observations, the formate first forms a formyl radical. The next step, where the formyl radical protonates the 3′-keto group of the substrate, is suggested to be rate limiting with a calculated total barrier of 19.9 kcal/mol, in reasonable agreement with the experimental rate-limiting barrier of 17 kcal/mol. Zero-point and entropy effects are found to be quite significant in lowering the barrier. The mechanism for the entire cycle is discussed in relation to known experimental facts.

I. Introduction

Ribonucleotide reductase (RNR) enzymes catalyze the reduction of ribonucleotides to deoxyribonucleotides that are needed for DNA synthesis and repair in all living cells. There are three classes of RNR, differing in protein structure but with the common property that they function via a free radical mechanism,[1−4] although they differ in the way the free radical is generated. Another common property is that redox-active metals are involved in the free radical generation. Class I RNR requires iron and oxygen for its tyrosyl radical generation. It is coded for by *nrdAB* genes in *Escherichia coli* and has an $\alpha_2\beta_2$ structure in which the larger α_2 protein has the active sites, and sites for allosteric regulation and the smaller β_2 protein has the iron/tyrosyl radical sites. Class II RNR has adenosylcobalamin as its radical generator and functions independently of oxygen. The anaerobic class III enzyme is destroyed by oxygen and an iron−sulfur cluster is required for the generation of its glycyl radical. The class III RNR enzymes consist of two proteins, NrdD and NrdG. The larger NrdD is the reductase where catalysis and allosteric regulation take place, whereas the smaller NrdG, the activase, contains an Fe_4S_4 cluster involved in glycyl radical generation together with the cofactor S-adenosyl methionine.[5−8] Formate is another cofactor needed for enzyme activity in the *E. coli* enzyme,[9] as well as in the T4 bacteriophage enzyme.[10] The glycine residue where the radical resides is located in the reductase.

All higher organisms have class I RNRs, whereas bacteria may have genes for any of the classes, sometimes for more than one. Class III RNRs are found in certain strictly or facultatively anaerobic bacteria under anaerobic conditions. A crystal structure of mutant NrdD reductase from bacteriophage T4 has been published.[11] Comparing it with the structure of the class I α_2 protein from *E. coli*,[12] similar folds have been observed. The glycine radical residue is located close to the active site in NrdD.

For class I RNRs, detailed models of its reaction mechanism have been proposed[13−19] (Figure 1), whereas less is known about the class III mechanism. Three cysteine residues close to the active site are essential for the class I enzyme activity:[20,21] Cys439 (*E. coli* numbering) proposed to form a thiyl radical which initially abstracts a hydrogen from the substrate, and Cys225 and Cys462, which deliver two reducing equivalents to the substrate. Only two of these are conserved in class III: Cys290 and Cys79 (bacteriophage T4 numbering), corresponding to Cys439 and Cys225, respectively. Cys462 is replaced by and corresponds to Asn311 in the class III enzyme. Cys79 and Cys290 have been shown to be necessary for catalysis of the class III enzyme.[10,22] Two additional residues proposed to be important for the catalytic mechanism in the class I RNR are missing in class III: Glu441 and Asn437, which are replaced by Met288 and Ser292 in class III, respectively. Clearly the catalytic mechanisms in the two classes have to differ at some point.[23]

A catalytic mechanism for the class III enzyme has been suggested[23] in which formate is the precursor of $\cdot CO_2^-$. This radical should serve as a reductant for the intermediate 3′-keto group formed on the substrate (Figure 2). The present study uses quantum chemical methods to probe the energetics of a feasible reaction mechanism for the class III RNRs. The mechanism is based on the known requirement for formate and the production of carbon dioxide in the reaction.[9] In essence it agrees with the structure-based mechanism discussed in ref 23.

II. Computational Details

All calculations were done using the GAUSSIAN 98 program.[24] The hybrid B3LYP functional[25,26] was used in the DFT calculations, as it is documented to perform well on systems of the present type.[17] The first step was to obtain optimized

* To whom correspondence should be addressed. Phone: +46-8-164621. Fax: +46-8-347817. E-mail: ps@physto.se.
[†] Department of Biophysics, Stockholm University.
[‡] The Scripps Research Institute.
[§] Department of Physics, Stockholm University.

10.1021/jp0107614 CCC: $20.00
Published on Web 06/09/2001

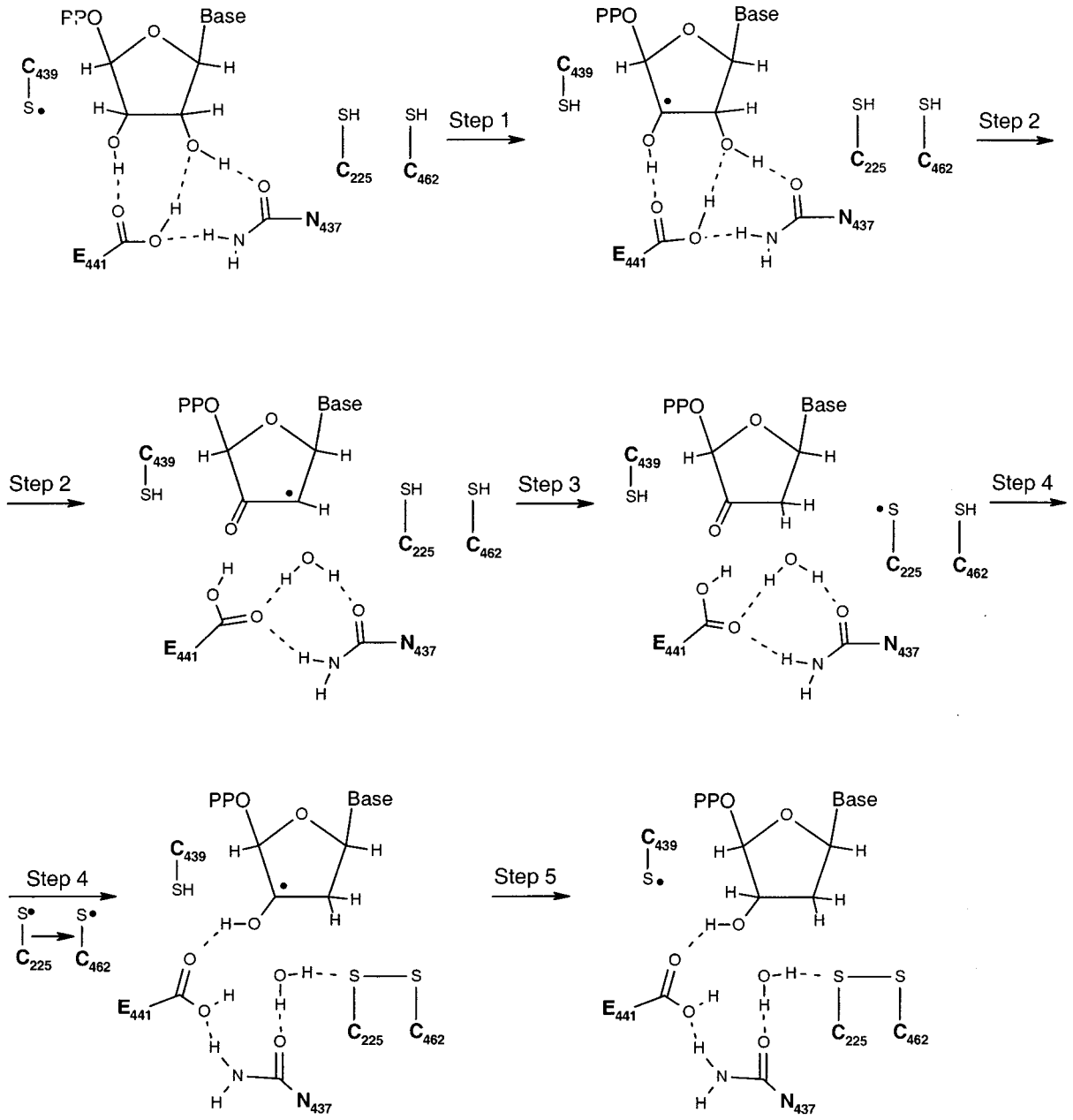

Figure 1. Previously suggested reaction mechanism for class I RNR.[4,17,18]

geometries, using the 6-311G(d,p) basis set, which is a triple-ζ basis set with d and p polarization functions. The relatively large basis set used should guarantee that also third row atoms such as sulfur, which is present in the calculations, are properly treated. In general, reaction energies are shown to be quite insensitive to the accuracy of the geometries,[27] implying that the choice of basis set is in fact more than adequate for geometry optimization purposes in the present system.

To obtain the zero-point vibrational energies, as well as temperature-dependent enthalpy and entropy effects (in future referenced as thermal effects), frequency calculations were performed at the optimized geometries using the same basis set. The frequency calculations also confirmed that the optimized geometries obtained have the desired properties (i.e., an energy minimum with no negative second derivatives, or in the case of a transition state, only one negative second derivative). The solvent effects on the energies at the optimized geometries were obtained by using the conductor-like solvation model COSMO,[28,29] also with the 6-311G(d,p) basis set. This is a continuum model, in which a cavity around the system of interest is surrounded by a polarizable continuum. In the present study, a dielectric constant of 4 was used, but a value of 80 was also used for the rate-limiting step for comparative purposes. Explicit geometry optimizations in the presence of solvent were not considered to be essential for the present system.[30]

To saturate the basis set effects on the energies, single-point calculations were performed at the optimized geometry using the 6-311+G(2d,2p) basis set. This triple-ζ basis set adds diffuse functions as well as two sets of polarization functions on all of the atoms. The spin and charge distributions reported are also given for these big basis set calculations, using the Mulliken population analysis. In general, the energy values discussed below include all of the effects described above. The exceptions are some model calculations done for comparative reasons on alternative structures, for which the energy values mentioned do not include dielectric and thermal effects, since the discussions there are very qualitative anyway.

To test the accuracy of the B3LYP method for the present systems, a few calculations were done at a higher level for the overall reaction energy of the reductive half-reaction. The

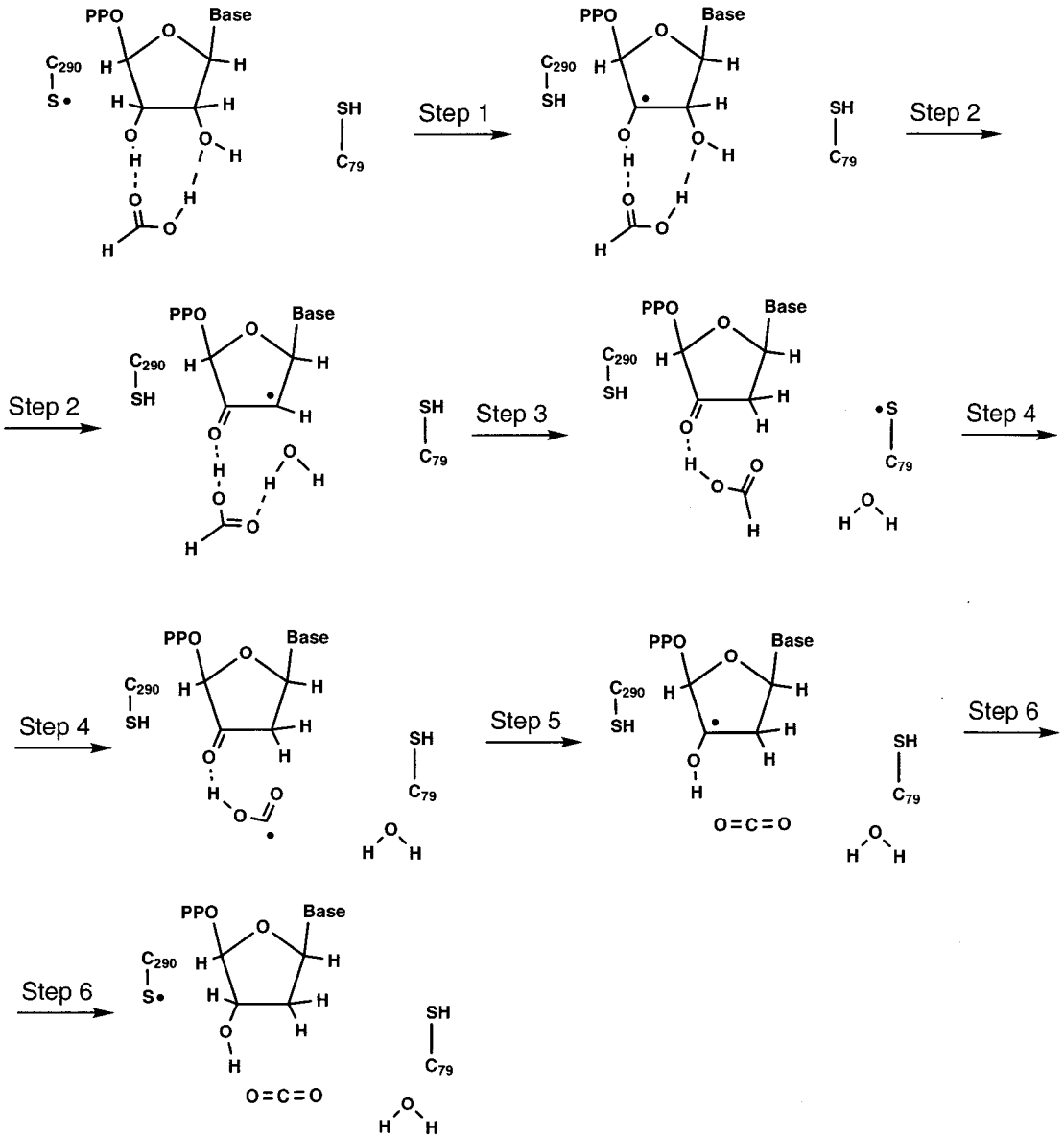

Figure 2. Proposed reaction mechanism for class III RNR (this study).

method used for these tests was the G2MS method,[31] which is similar to the original G2MP2 method[32] except that somewhat smaller basis sets are used, the 6-31G* basis for the CCSD(T) calculations[33] and the 6-311+G(2df,2p) basis for the MP2 calculations. B3LYP geometries as described above were used, and the critical C−H bond energy of formic acid and the S−H bond energy in $SH(CH_3)$ (as a model for cysteine) were investigated. The G2MS C−H bond energy of formic acid is 0.4 kcal/mol stronger than the one obtained at the B3LYP level. A similar trend is seen for the S−H bond energy of cysteine, which is 0.7 kcal/mol stronger at the G2MS level. The conclusion is that the B3LYP method does extremely well for both of these energies, and the B3LYP results for the model reactions discussed below should therefore be reasonably accurate.

III. Results and Discussion

The previously proposed mechanism for aerobic RNR,[17,18] see Figure 1, constitutes the starting point for the present investigation of the anaerobic mechanism. The aerobic mechanism is a modification after theoretical studies of the one proposed by Stubbe et al. based on experimental results.[4] It starts where the (*E. coli*) Cys439 radical has been created, and the anaerobic mechanism therefore starts where the analogous (T4) Cys290 radical has been created. The processes leading to the formation of these radicals are substantially different in the two enzymes (cf. refs 1−4) and will not be discussed further here. The first steps, leading from the Cys290 radical to the formation of the 3′-keto group at the ribose ring, are suggested here to be very similar to the aerobic mechanism. The main differences should be that the role of Glu441 in the aerobic *E. coli* enzyme is taken by solvent formate and that asparagine corresponding to Asn437 is missing in the anaerobic enzyme. These steps will therefore be slightly modified as discussed further in subsection d. An overview of the mechanism for the anaerobic enzyme presented here is shown in Figure 2 with the numbering of the involved residues. The point where the anaerobic and aerobic mechanisms start to deviate substantially is when the stable nonradical 3′-keto form of the ribose ring has been formed after step 3 in Figure 1 and Figure 2. At this stage, the Cys79 radical should also have been created.

At the point where the Cys79 radical and the keto group have been created it is suggested that the formate comes into the

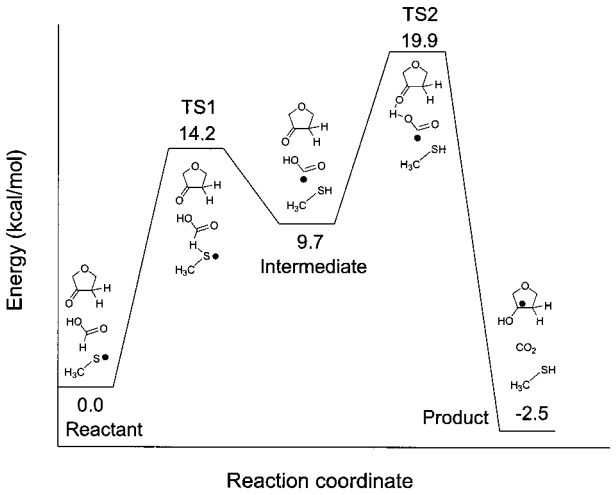

Figure 3. Energy diagram for the steps studied here in the reaction mechanism of class III RNR.

reaction as a hydrogen donor, here modeled as formic acid. The formic acid is also proposed to have another function, as discussed later. The choice of formic acid rather than formate as a model is made here mainly because both a proton and a formate are needed in the mechanism at some stage. It should be added that this is a requirement in all mechanisms suggested so far, including the structure-based mechanism of Eklund and Fontecave[23] and the one in Figure 1. The question is only where this required proton should be placed. Since it is also required that it is easily accessible by the 3′-keto group and the formate is in this region, the proton is simply placed there in the present model.

a. Creation of a Formyl Radical. The calculated energetics for the creation of the formyl radical is shown as the initial step in Figure 3. In this step the Cys79 radical abstracts the C-bound hydrogen from formic acid, leading to a formyl radical intermediate (step 4, Figure 2). This step has a calculated reaction barrier and endothermicity of 14.2 and 9.7 kcal/mol, respectively. Figure 4 shows the TS1 structure, with important bond lengths and spin distributions displayed. By modeling in a ribose group into the crystal structure of class III RNR[11] so that it corresponds to the aerobic case, it can be seen that the Cys79 residue is not far away from the 2′ site of the ribose ring. Assuming that the small formic acid (or formate) can move freely in the region, the different groups might very well orient themselves relative to each other in the fashion described by the figure. The crystal structure of class III RNR does therefore not contradict the transition structure here obtained.

The energetics of the creation of the formyl radical is probably the most important result of the present study. The creation of a formyl radical has been suggested before for this step,[23] but the question remained as to how this radical could exist in the protein without causing significant damage. One answer to this question is that the formyl radical exists only at a high energy of 9.7 kcal/mol (Figure 3). This means that for the formyl radical to create any damage it needs to be involved in a reaction with an exothermicity of at least 10 kcal/mol. Only hydrogen abstractions from the amino acids tyrosine, tryptophane, cysteine, and glycine fall into this category. The closest residue of this type is Cys79, which, if it reacted with the formyl radical, only would go back to the start of this step. Tyr581 and Tyr441 are also relatively close. However, in order for the formyl radical to reach one of these tyrosines, the hydrogen bond of the formyl radical OH to the substrate 3′-O (see Figure 2 after step 4) would need to be broken. This hydrogen bond is calculated to be

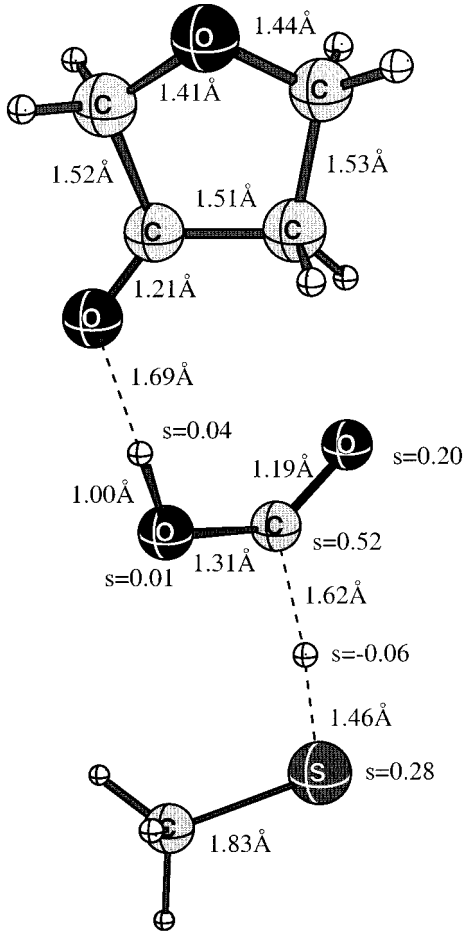

Figure 4. Optimized transition state (TS1) for formation of the formyl radical.

surprisingly strong with 10.5 kcal/mol. If this energy is added to the energy of the formyl radical of 9.7 kcal/mol, an absolute lower limit for the barrier of 20 kcal/mol can be estimated for the reaction with Tyr581 or Tyr441. Normally, also the reaction by itself would lead to an additional barrier; in the case of tyrosine, the cleavage of the O−H bond. The same type of barrier would appear for any reaction where the formyl radical would migrate away from the active site. The unusually strong hydrogen bond of the formyl radical OH should therefore be enough to hold the radical in place during the reaction and prevent it from straying away, until the second step of the reaction is finished. It should again be noted that the strong hydrogen bond to the formyl radical found depends on the use of a formic acid model. What would happen in the case of a negatively charged formate anion model is less clear. However, in this case also, the negative charge should lead to strong hydrogen bonds and strongly limit the motional flexibility of the radical.

The different energy contributions for the present mechanism are shown in Table 1. As can be seen there, the zero-point vibrational energy effect is fairly large, lowering the barrier with 3.5 kcal/mol, which is expected for a hydrogen atom transfer step. A large deuterium kinetic isotope effect is also expected. The thermal effects, on the other hand, raise the barrier by 0.9 kcal/mol but, as it turns out, this is the only point where they work against the reaction. At the intermediate state, all of the spins reside on the formyl radical (Figure 5). The thermal effects for the creation of the product radical are substantial, lowering the energy of this state by 2.6 kcal/mol. The thermal effects can therefore be regarded as one of the main forces driving this

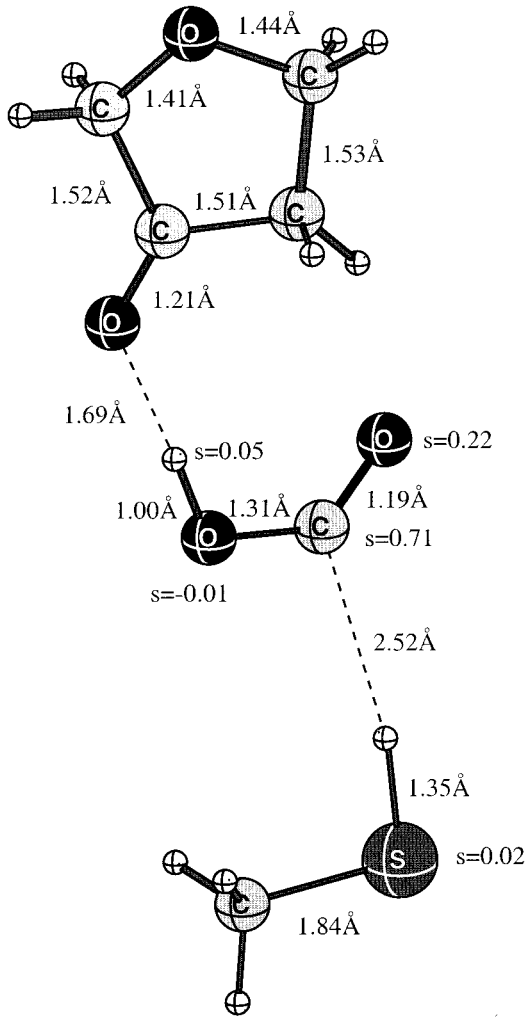

Figure 5. Optimized structure for the intermediate formyl radical state.

TABLE 1: Energies for the Different Points along the Reaction Path (Figure 3) for the Formation of the Formyl Radical and of Carbon Dioxide

		reactant	TS1	intermediate	TS2	product
A	B3LYP energy	0.00	16.98	14.51	27.65	1.52
B	solvation energy		−0.26	−0.25	−1.81	0.77
C	zero point energy		−3.49	−1.93	−4.89	−1.91
	A+B+C	0.00	13.23	12.33	20.94	0.38
D	entropy		1.01	−3.45	−1.42	−3.16
E	thermal enthalpy		−0.09	0.81	0.35	0.24
	A+B+C+D+E	0.00	14.16	9.69	19.87	−2.54

reaction forward, as can be expected considering that a nearly free carbon dioxide is formed at the end, affecting the entropy of the system. Solvent effects are still negligible so far in the reaction.

b. Hydrogen Abstraction by Deoxyribose-3′-O. In the step after the formyl radical has been created, the 3′-keto-deoxyribose ring is suggested to abstract the O-bound hydrogen atom from the formyl radical (step 5, Figure 2). This step involves a barrier of 10.2 kcal/mol, which gives a total barrier of 19.9 kcal/mol relative to the resting state with the Cys79 radical (Figure 3 and Table 1). Figure 6 shows the structure and spin distribution for TS2. This barrier would indicate a rate of only 10^{-3} s^{-1}, which is slower than the measured rate of the substrate reaction of 3 s^{-1},[3] but not outside reasonable error limits for a reaction of this type. The experimental rate corresponds to a rate-limiting barrier of about 17 kcal/mol, which indicates an error in the calculated value of 2.9 kcal/mol. The difficulty to reach an

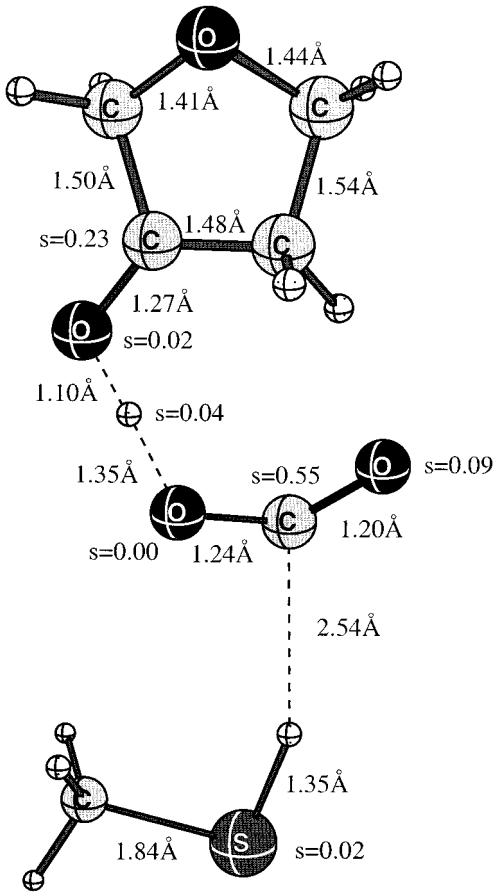

Figure 6. Optimized transition state (TS2) for formation of carbon dioxide from the formyl radical.

accurate value for this barrier is clear when the different contributions, shown in Table 1, are analyzed. Quite remarkably, the barrier height computed from the B3LYP energies alone is as high as 27.7 kcal/mol. For the smaller basis set used in the geometry optimization the barrier is even higher with 28.4 kcal/mol, as much as 11.4 kcal/mol higher than the upper limit given by experiments of 17 kcal/mol. At this stage of the calculations, the conclusion was therefore that this mechanism is most probably not the correct one. However, when the zero-point vibrational effects were calculated and found to decrease the barrier by as much as 4.9 kcal/mol, the barrier of 22.8 kcal/mol can no longer be entirely ruled out. The zero-point vibrational energy effect compared to the formyl radical is somewhat smaller with 3.0 kcal/mol. Adding also the remaining effects leads to an additional decrease of the barrier. The calculated thermal effects using an harmonic Hessian lower the barrier by 1.1 to 21.7 kcal/mol, which could be an underestimate of the actual thermal effect, see below. Addition of the dielectric effects of −1.8 kcal/mol leads to the final best estimate of 19.9 kcal/mol. These effects taken together, all of them favoring the reaction, thus help lowering the barrier by a substantial amount of 7.8 kcal/mol. The final deviation to experiments of 2.9 kcal/mol is quite reasonable using the B3LYP method. The available experience so far on enzymes using this method is that estimated energy barriers tend to be slightly too high.[34]

A few calculations were done to study the sensitivity of the barrier to the model used. First, the choice of dielectric constant is somewhat arbitrary and leads to some uncertainty. If water can easily access the active site, a dielectric constant higher than 4 could be expected. As an extreme, a dielectric constant of 80 was used leading to a lowering of the barrier by 3.2 kcal/

mol, which is 1.7 times more than when a dielectric constant of 4 is used, indicating a small but non-negligible dependence on the value of the dielectric constant. Another possible source for lowering the barrier further could come from the presence of Asn311, a residue that is known to be conserved in all class III RNR species[11] close to Cys79. In the previous study of aerobic RNR,[17] the presence of an asparagine (at an another place) was shown to lower the computed barrier for one step by as much as 4.6 kcal/mol. A model calculation was therefore performed, where an asparagine was included at the position of Asn311 in anaerobic RNR, modeled by $CHONH_2$ hydrogen bonded to the Cys79 radical. However, it turns out that this hydrogen bond becomes only about 0.5 kcal/mol stronger once the cysteine radical abstracts a hydrogen atom. The intermediate state will then be lowered by the same amount with respect to the starting point, and with that the following states as well (including TS2). The role of water molecules at the active site has also been investigated. Adding a water molecule between the formyl radical and 3′-O of the substrate will give it a role in the hydrogen atom transfer. Small model calculations of this effect indicate a lowering of the barrier by about 1 kcal/mol. In trying to lower the barrier, a concerted mechanism was also sought where both hydrogen atoms leave the formic acid simultaneously without any intermediate state being formed. The conclusion drawn after an extensive search is that such a concerted transition state does not exist. In all of these attempts, the transition state geometry optimizations always ended up in TS1, TS2, reactant, or product. The graph in Figure 3 also shows that the intermediate state is a distinct one between the two transition states, 4.5 kcal/mol below TS1, further strengthening the conclusion that no concerted transition state is to be found. In summary, it is clear that many factors even if they are all quite small, could contribute to a lowering of the barrier for this step and further improve the agreement with experiments.

Another question for this reaction step concerns whether the formyl radical remains in its trans position with respect to the now missing hydrogen, or flips over to the cis position when it turns into a radical. The trans formic acid is 4.8 kcal/mol lower in energy than its corresponding cis form, whereas the cis formyl radical is calculated to be 1.2 kcal/mol more favorable in energy than the trans formyl radical. However, small model calculations including only the ribose ring and the formyl radical indicate that the hydrogen abstraction transition state (corresponding to TS2) for the cis structure is about 1.5 kcal/mol above the one for the trans structure (TS2) in energy. It is therefore concluded that the formyl radical reaction will have to pass over transition state TS2 with the formyl radical in its trans conformation, even though the isolated formyl radical is more stable in its cis conformation.

A few words should be mentioned about the search for TS2 because it was not trivial. To approach the transition state from the reactant formic acid side, the 3′-O−H distance was frozen at different values during the geometry optimizations, while all other geometrical parameters were allowed to relax. The potential energy plotted against the 3′-O−H distance, shows that the energy surface is steadily uphill with decreasing distance, ending in a sudden drop in energy when the formyl radical turns into carbon dioxide. In this region, the step size has to be very small or the transition state will be missed. The same happens when the transition state is approached from the product side. If the geometry for the Hessian evaluation was chosen only slightly away from the final correct geometry, the transition state optimization would fall back into either reactant or product, which happened in several early attempts. Because the sudden drop in energy along the reaction path could be explained by an early proton transfer during this step, followed by an electron transfer somewhat later, a partial charge separation at TS2 is thus plausible, even though the net result of the entire step is a transfer of a hydrogen atom. From the dielectric effect of −1.6 kcal/mol on TS2 with respect to the intermediate state (see Table 1), some charge separation can be noted. However, the Mulliken populations at the final transition state indicate that the accepting oxygen together with the transferring proton get an increase in charge of only 0.08 compared to the starting structure. The reaction mechanism is still probably best described as hydrogen atom transfer.

c. Formation of Carbon Dioxide. The final part of the step where formic acid (or formate) reacts with the substrate is the formation of carbon dioxide (step 5, Figure 2). The product state is calculated to be 22.4 kcal/mol below TS2 (Figure 3), making the whole reaction exothermic by 2.5 kcal/mol. Thermal effects are expected to be quite large since a nearly free carbon dioxide is produced. Even though these effects were computed to be substantial, favoring the forward reaction by 2.9 kcal/mol, this is smaller than expected. Not enough information is available about the accuracy of thermal effects calculated by the use of harmonic Hessians, but from the present results it appears that they may be slightly underestimated. Actual thermal effects larger than the calculated ones would also contribute to lowering the barrier height, see above.

A point of technical importance is worth making in connection with the formation of carbon dioxide. DFT calculations are usually quite insensitive to the basis set size,[34] and qualitatively reasonable results are generally found at the double-ζ level. Since the initial calculations in the investigation of a new mechanism are often made at this level, it is tempting to draw conclusions at this stage of the calculations. However, this will not work in the present case. At the double-ζ level, the sum of the C−H bond strength of formic acid and the O−H bond strength of the formyl radical is found to be as much as 11.6 kcal/mol too strong compared to the final basis set results. This leads to a final endothermicity of the formation of carbon dioxide of almost 10 kcal/mol compared to the final basis set result of an exothermic reaction by 2.5 kcal/mol. A large part of this problem stems from the requirement for polarization functions to describe the two double bonds of carbon dioxide. Nevertheless, on the other hand, the geometries obtained at the double-ζ level are sufficiently accurate. Large basis sets for the geometries were used anyway to be on the safe side.

d. The Entire Substrate Mechanism for Anaerobic RNR. As indicated above, the reaction between the formic acid and the ribose ring is the only part of the substrate mechanism which is expected to deviate substantially from the mechanism of aerobic RNR. To obtain a suggestion for the entire substrate mechanism, all that needs to be done is essentially to patch this part into the previously suggested mechanism for aerobic RNR, see Figure 1. The total reaction mechanism for anaerobic RNR, from the deoxyribose ring to the ribose ring, is described in Figure 2, where previous works on the aerobic enzyme[17,18] have been linked with the present study. There are some slight differences in the studies worth mentioning. Previous studies used a double-ζ basis set for geometry optimizations (except for the sulfur atom) and frequency calculations, and the solvent effect was calculated with the SCI−PCM method.[35] The frequency calculations were done at the HF level with the zero-point vibrational energies scaled by 0.9 as usual. The thermal and solvent effects were all found to be small and less accurate,

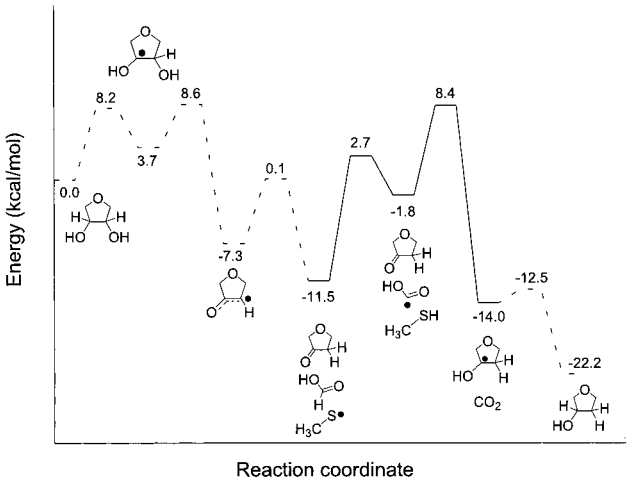

Figure 7. The suggested reaction mechanism for anaerobic class III RNR.

and the reported values were without these effects included. These small variations, however, should not change the general picture of the reaction mechanism. The possible energetic deviations should not be larger than a couple of kcal/mol. An another difference between the aerobic and anaerobic enzymes is structural. In class III RNR, any equivalents of class I RNR Glu441 and Asn437 are missing. In the case of Glu441, the previous studies had used formic acid as a model for the glutamic acid. In class III RNR, there are real formic acids (or formate) in the enzyme. The role of the formate is therefore proposed to be 2-fold in class III RNR: it replaces the function of Glu441 as a hydrogen bonding partner in the substrate and it acts as a hydrogen donor for the reaction. This makes the part of the results found for class I RNR regarding Glu441 equally valid for the class III system with formic acid. The lack of Asn437 has consequences already studied previously.[17] It raises the barrier of the first step in the reaction compared to class I RNR, around 8.2 kcal/mol compared to 7.2 kcal/mol, with an endothermicity of 3.7 kcal/mol compared to 2.2 kcal/mol. The next step, where a water molecule leaves the substrate, is slightly more affected by the lack of Asn437: a barrier of 4.9 kcal/mol compared to 0.3 kcal/mol and an exothermicity of 11.0 kcal/mol compared to 10.7 kcal/mol. However, this should have no consequence for the entire reaction rate because the resulting barriers for these steps are still lower than the rate-limiting barrier of 19.9 kcal/mol.

The present mechanism is consistent with the work of Andersson et al.,[10] in which they showed by site-directed mutagenesis that Cys79 and Cys290 are essential for the reaction mechanism. Also, a study by Mulliez et al.,[9] in which they replaced the C-bound hydrogen in formate with tritium, is consistent with the present mechanism. They found that tritium eventually ends up in water and not in the substrate. In the current mechanism, the C-bound hydrogen ends up in the protein at Cys79. The agreement between experiments and theory depends on the rate of proton exchange between Cys79 and water and requires that this is faster than the rate-limiting step of the substrate reactions. If the rate of proton exchange for Cys79 were slower than the rate limiting step, tritium would be found in the substrate after a few turnovers. The exchange rate for protons between water and the cysteine side chain has been studied experimentally for the isolated cysteine amino acid,[36] and a rate of 1400 s^{-1} was found, substantially faster than the rate-limiting step of anaerobic RNR. However, the same process was also recently studied theoretically, and the rate was found to be strongly dependent on the number of water molecules that can directly access the cysteine.[30] It is not obvious from the structure of class III RNR how many water molecules can effectively interact with Cys79, but formic acid could also take the role of water in this process. It is clear nevertheless that the rate of proton exchange for Cys79 is likely to be substantially faster than the rate-limiting step of the substrate reactions. Therefore, the present study agrees with the tritium experiment that tritium should be found in water and not in the substrate. Also, the carbon itself in formate has been labeled with ^{14}C,[9] and it is found to end up in carbon dioxide, as it does in the current mechanism.

As discussed in the beginning of this section, the proton required to protonate the 3′-keto group of the substrate is in the present model placed at the formate to make a formic acid. To investigate if the proton could possibly enter at a later stage in the mechanism, a few additional calculations were performed. In the first of these, it was studied whether the presence of the proton is necessary in the first step in Figure 3. This does not appear to be the case. For a model without this proton, which is thus negatively charged, the endothermicity of the first step becomes 7.6 kcal/mol, which is actually somewhat lower than with the proton present. The barrier appears also to be somewhat lower without the proton. Because the first step is not rate-limiting, the consequence of the presence of the proton here is, at most, marginal. However, in the second rate-limiting step in Figure 3, the presence of the proton is very important. Calculations without the proton gave a strongly endothermic reaction for the second step of 13.0 kcal/mol, in contrast to the case with the proton present, which is exothermic by 12.2 kcal/mol, as described above. The conclusion is therefore that the proton must enter the 3′-keto group region *before* the second rate-limiting step. Precisely how this occurs is one of the major remaining questions in the mechanism of anaerobic RNR, and should be adressed in future studies.

IV. Conclusions

A mechanism for the substrate reactions in class III RNR has been suggested based on B3LYP calculations. This mechanism is based on the recently published alanine mutant structure of RNR for bacteriophage T4[11] and is consistent with this structure. The mechanism differs from the previous one for aerobic class I RNR,[17,18] only in the steps where carbon dioxide is formed from solvent formate. This part replaces the part in the aerobic mechanism where an S−S bond is formed between two cysteines. The formation of carbon dioxide is suggested to go over a formyl radical, as has also been proposed recently on the basis of structural information.[23] An important question in this context is how a formyl radical can exist in the enzyme without causing damage. This question is partly answered by the calculations, which show that the formyl radical exists only in an unstable state almost 10 kcal/mol above the stable Cys79 radical. This means that the formyl radical can only possibly cause damage if it is involved in reactions with exothermicities higher than 10 kcal/mol. From the X-ray structure it appears clear that no reaction of this type is possible that would be harmful for the enzyme. The Cys79 radical could, of course, be formed, but this is obviously harmless since it must appear anyway. Formation of the Tyr441 or Tyr581 radicals may also be possible but there is no reason why these radicals should be harmful. As a further protection of the formyl radical, it is strongly hydrogen bonded by about 10 kcal/mol. This bond has to be broken if the radical should migrate away to an another region, and this would place it at an energy about 20 kcal/mol

above the Cys79 radical if this hydrogen bond is not replaced by an equally strong bond. In that case there would still be a barrier of 20 kcal/mol for it to reach this other position, which should also prevent harmful reactions because the rate-limiting barrier for the substrate reactions is only 17 kcal/mol.

When the formyl radical has been created, it is suggested to lose its remaining hydrogen to the substrate and carbon dioxide will be formed. There are many effects which all contribute to lowering the barrier for the formation of carbon dioxide, which is proposed to be the rate-limiting step of the entire substrate reaction. The main factor lowering the barrier is the decrease of zero-point vibrational energy by as much as 4.9 kcal/mol. Entropy and other thermal effects obviously also favor this reaction since the carbon dioxide product is nearly free. The dielectric effects finally give a small contribution decreasing the barrier. The final barrier of 19.9 kcal/mol is in reasonably good agreement with the experimental rate-limiting barrier of 17 kcal/mol, considering the normal errors for the B3LYP method.

The presently suggested mechanism is consistent with experimental findings.[9,10] For example, Cys79 and Cys290 are known to be essential for the reaction mechanism. In the present mechanism, Cys290 starts the whole reaction by abstracting the 3′-O hydrogen, and Cys79 is involved in creating the formyl radical. Also, tritium from labeled formate is found experimentally in the solvent and not in the substrate. As can be seen in Figure 2, the tritium would here first go to Cys79 and later exchange with the solvent, at an estimated rate which is considerably faster than the rate-limiting step of the reaction. The ^{14}C from labeled formate is found in the product carbon dioxide, which is also consistent with the present mechanism. The mechanism suggested here for anaerobic RNR may also be of relevance for the catalytic mechanism of the enzyme pyruvate formate lyase (PFL), which is structurally similar to the RNR structures.[37,38] Also PFL carries a glycyl radical,[39] but in this case formate is a product of the catalytic reaction which rearranges pyruvate. In summary, the present energetics and other agreement with experiments indicate that the suggested mechanism is a feasible one. However, it should be made clear that this does not prove that the mechanism is the right one. Future work may still show that other mechanisms are even more favorable.

V. Acknowledgments

We thank Prof. Pär Nordlund, Dr. Derek Logan, and Prof. Britt-Marie Sjöberg for valuable discussions and technical assistance. This work was supported by grants from Swedish Natural Science Council, the Swedish Foundation for Strategic Research, and EU-TMR network under contract no. ERBFMRXCT98027.

References and Notes

(1) Reichard, P. *Science* **1993**, *260*, 1773.
(2) Jordan, A.; Reichard, P. *Annu. Rev. Biochem.* **1998**, *67*, 71−98.
(3) Sjöberg, B.-M. *Struct. Bonding* **1997**, *88*, 139−173.
(4) Stubbe, J.; van der Donk, W. A. *Chem. Rev.* **1998**, *98*, 705−762.
(5) Young, P.; Andersson, J.; Sahlin, M.; Sjöberg, B.-M. *J. Biol. Chem.* **1996**, *271*, 20770−20775.
(6) Ollagnier, S.; Mulliez, E.; Schmidt, P. P.; Eliasson, R.; Gaillard, J.; Deronzier, C.; Bergman, T.; Gräslund, A.; Reichard, P.; Fontecave, M. *J. Biol. Chem.* **1997**, *272*, 24216−24223.
(7) Tamarit, J.; Gerez, C.; Meier, C.; Mulliez, E.; Trautwein, A.; Fontecave, M. *J. Biol. Chem.* **2000**, *275*, 15669−15675.
(8) Liu, A.; Gräslund, A. *J. Biol. Chem.* **2000**, *275*, 12367−12373.
(9) Mulliez, E.; Ollagnier, S.; Fontecave, M.; Eliasson, R.; Reichard, P. *Proc. Natl. Acad. Sci. U.S.A.* **1995**, *92*, 8759−8762.
(10) Andersson, J.; Westman, M.; Sahlin, M.; Sjöberg, B.-M. *J. Biol. Chem.* **2000**, *275*, 19449−19455. Bodevin, S.; Sjöberg, B.-M., personal communication.
(11) Logan, D. T.; Andersson, J.; Sjöberg, B.-M.; Nordlund, P. *Science* **1999**, *283*, 1499−1504.
(12) Uhlin, U.; Eklund, H. *Nature* **1994**, *370*, 533−539.
(13) Stubbe, J. *Adv. Enzymol. Relat. Areas Mol. Biol.* **1990**, *63*, 349−419.
(14) Mao, S. S.; Holler, T. P.; Yu, G. X.; Bollinger, J. M.; Booker, S.; Johnston, M. I.; Stubbe, J. *Biochemistry* **1992**, *31*, 9733−9743.
(15) Siegbahn, P. E. M.; Blomberg, M. R. A.; Crabtree, R. H. *Theor. Chem. Acc.* **1997**, *97*, 289−300.
(16) Siegbahn, P. E. M.; Eriksson, L.; Himo, F.; Pavlov, M. *J. Phys. Chem. B* **1998**, *102*, 10622−10629.
(17) Siegbahn, P. E. M. *J. Am. Chem. Soc.* **1998**, *120*, 8417−8429.
(18) Himo, F.; Siegbahn, P. E. M. *J. Phys. Chem.* **2000**, *104*, 7502−7509.
(19) Zipse, H. *Chem. Eur. J.* **1999**, *5*, 3046−3054.
(20) Åberg, A.; Hahne, S.; Karlsson, M.; Larsson, A.; Ormö, M.; Åhgren, A.; Sjöberg, B.-M. *J. Biol. Chem.* **1989**, *264*, 12249−12252.
(21) Mao, S. S.; Yu, G. X.; Chalfoun, D.; Stubbe, J. *Biochemistry* **1992**, *31*, 9752−9759.
(22) Olcott, M. C.; Andersson, J.; Sjöberg, B.-M. *J. Biol. Chem.* **1998**, *273*, 24853−24860.
(23) Eklund, H.; Fontecave, M. *Structure* **1999**, *7*, R257−R262.
(24) Frisch, M. J.; Trucks, G. W.; Schlegel, H. B.; Scuseria, G. E.; Robb, M. A.; Cheeseman, J. R.; Zakrzewski, V. G.; Montgomery, J. A., Jr.; Stratmann, R. E.; Burant, J. C.; Dapprich, S.; Millan, J. M.; Daniels, A. D.; Kudin, K. N.; Strain, M. C.; Farkas, O.; Tomasi, J.; Barone, V.; Cossi, M.; Cammi, R.; Mennucci, B.; Pomelli, C.; Adamo, C.; Clifford, S.; Ochterski, J.; Petersson, G. A.; Ayala, P. Y.; Cui, Q.; Morokuma, K.; Malick, D. K.; Rabuck, A. D.; Raghavachari, K.; Foresman, J. B.; Cioslowski, J.; Ortiz, J. V.; Stefanov, B. B.; Liu, G.; Liashenko, A.; Piskorz, P.; Komaromi, I.; Gomperts, R.; Martin, R. L.; Fox, D. J.; Keith, T.; Al-Laham, M. A.; Peng, C. Y.; Nanayakkara, A.; Gonzalez, C.; Challacombe, M.; Gill, P. M. W.; Johnson, B.; Chen, W.; Wong, M. W.; Andres, J. L.; Head-Gordon, M.; Replogle, E. S.; Pople, J. A. 1998 *Gaussian 98*, Gaussian Inc.: Pittsburgh, PA.
(25) Becke, A. D. *Phys. Rev.* **1988**, *A38*, 3098. Becke, A. D. *J. Chem. Phys.* **1993**, *98*, 1372. Becke, A. D. *J. Chem. Phys.* **1993**, *98*, 5648.
(26) Stevens, P. J.; Devlin, F. J.; Chablowski, C. F.; Frisch, M. J. *J. Phys. Chem.* **1994**, *98*, 11623.
(27) Bauschlicher, C. W., Jr.; Ricca, A.; Partridge, H.; Langhoff, S. R. In *Recent Advances in Density Functional Methods, Part II*; Chong, D. P., Ed.; World Scientific Publishing Company: Singapore, 1997, p 165.
(28) Miertus, S.; Scrocco, E.; Tomasi, J. *Chem. Phys.* **1981**, *114*, 117. Miertus, S.; Tomasi, J. *Chem. Phys.* **1982**, *65*, 239. Cossi, M.; Barone, V.; Cammi, R.; Tomasi, J. *Chem. Phys. Lett.* **1996**, *255*, 327.
(29) Barone, V.; Cossi, M. *J. Phys. Chem.* **1998**, *102*, 1995−2001.
(30) Prabhakar, R.; Blomberg, M. R. A.; Siegbahn, P. E. M. *Theor. Chem. Acc.* **2000**, *104*, 461−470.
(31) Froese, D. J.; Humbel, S.; Svensson, M.; Morokuma, K. *J. Phys. Chem.* **1997**, *101*, 227.
(32) Curtiss, L. A.; Raghavachari, K.; Pople, J. A. *J. Chem. Phys.* **1993**, *98*, 1293.
(33) Pople, J. A.; Head-Gordon, M.; Raghavachari, K. *J. Chem. Phys.* **1987**, *87*, 5968.
(34) Siegbahn, P. E. M.; Blomberg, M. R. A. *Chem. Rev.* **2000**, *100*, 421−437.
(35) Wiberg, K. B.; Rablen, P. R.; Rush, D. J.; Keith, T. A. *J. Am. Chem. Soc.* **1995**, *117*, 4261. Wiberg, K. B.; Keith, T. A.; Frisch, M. J.; Murcko, M. *J. Phys. Chem.* **1995**, *99*, 9072.
(36) Liepinsh, E.; Otting, G. *Magn. Reson. Med.* **1996**, *35*, 30−42.
(37) Leppänen, V.; Merckel, M. C.; Ollis, D. L.; Wong, K. K.; Kozarich, J. W.; Goldman, A. *Structure* **1999**, *7*, 733−744.
(38) Becker, A.; Fritz-Wolf, K.; Kabsch, W.; Knappe, J.; Schultz, S.; Wagner, A. *Nature Struct. Biol.* **1999**, *6*, 969−975.
(39) Wagner, A.; Frey, M.; Neugebauer, F.; Schäfer, W.; Knappe, J. *Proc. Natl. Acad. Sci. U.S.A.* **1992**, *89*, 996−1000.